Supplementary Information

cis,cis-Muconic acid isomerization and catalytic conversion to biobased cyclic-C_6-1,4-diacid monomers

Jack M. Carraher,[a,b] Toni Pfennig,[a,b] Radhika Giri Rao,[a,b] Brent H. Shanks,[a,b] and Jean-Philippe Tessonnier*[,a,b]

[a.] *Department of Chemical and Biological Engineering, Iowa State University, Ames, IA 50011, USA. E-mail: tesso@iastate.edu*
[b.] *NSF Engineering Research Center for Biorenewable Chemicals (CBiRC), Ames, IA 50011, USA.*

email: tesso@iastate.edu

Method to differentiate between loss of ^{1}H NMR signal due to D-incorporation/H-loss or degradation

Data was processed in two ways for correction of signal loss due to deuterium incorporation/proton loss. Method 1 (eq S1 – S5) assumes 1) no degradation (*e.g.* only *ct*MA, Mlac, and lac 2 exist in solution, therefore, signal loss is due solely to Scheme S1) and 2) equal incorporation of D in Mlac and Lac2.

$[MA]_{total} = \Sigma$ [MA isomers] eq S1

$K_3 = [Lac2] / [Mlac]$ eq S2

$[Lac]_{total} = [Mlac] + [Lac2] = [MA]_{total} - [ct\text{MA}]$ eq S3

$[Lac]_{total} = [Mlac] + [Lac2] = (1/K_3 + 1)[Lac2]$ eq S4

$[Lac2] = [Lac]_{total}/(1/K_3 + 1)$ eq S5

Method 2 allows for degradation of MA (eq S6 – S8). Method 2 assumes 1) that degradation is sufficiently slow and equilibrium K_3 is not perturbed and 2) that deuterium incorporation is equal in both Mlac and Lac2. The first assumption is easily justified when considering that the [Mlac]/[Lac2] ratio does not change once equilibrium is achieved (Figure S1). The latter assumption is not entirely accurate, however, must be made. The result is a slight overestimation of [Mlac] and [Lac2].

$MA\text{-}D_{signal\ at\ time\ t} = MA_{initial\ signal} - MA_{total\ signal\ at\ time\ t}$ eq S6

$[Mlac]_{corrected} = (1 + \%\ MA\text{-}D_{signal})[Mlac]_{measured}$ eq S7

$[Lac2]_{corrected} = (1 + \%\ MA\text{-}D_{signal})[Lac2]_{measured}$ eq S8

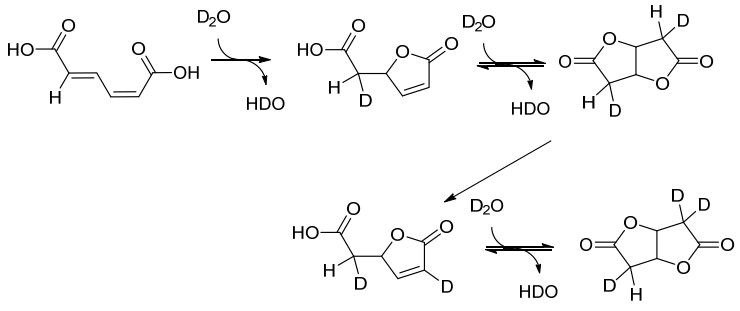

Scheme S1. Deuterium incorporation and proton loss during reversible lactonisation.

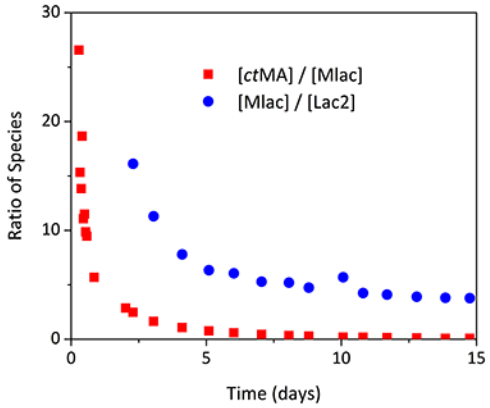

Figure S1. Relative concentrations as a function of time for Isomerization at 75 °C.

Application of both corrections is shown in Figure S2a-d. The fit of both models to kinetic traces obtained at 75 °C indicates that no degradation has occurred at these temperatures. However, the deviation of corrected experimental points from simulation at 95 °C indicates degradation of one or multiple MA species.

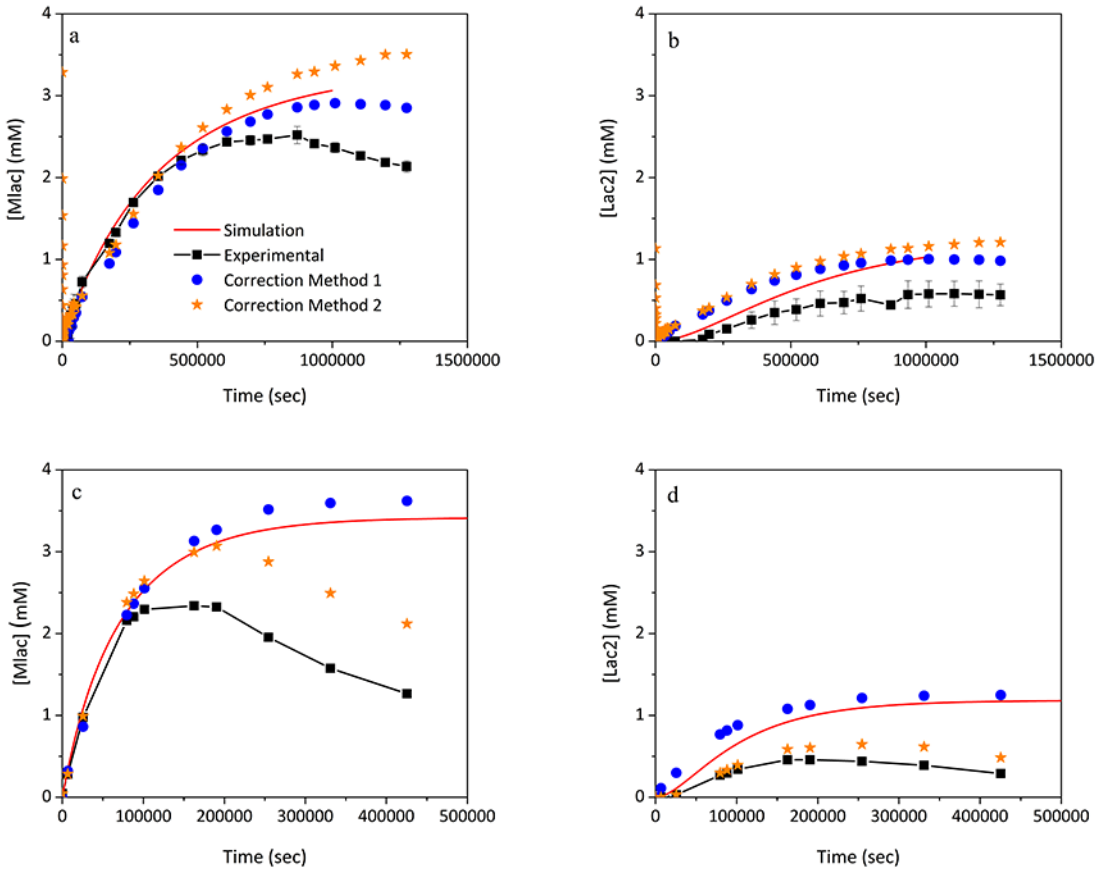

Figure S2. Plots of [Mlac] and [Lac2] as a function of time. Experimental data, corrected experimental data utilizing both Method 1 and Method 2 described above, and simulated data are shown for reactions at a & b) 75 °C and c & d) 95 °C.

Method for estimating elementary rate constants and acid dissociation constants by simplified fitting of experimental k_{obs} as a function of pH

Attempts to measure Ka_1 and Ka_2 for both *cc*MA and *ct*MA by titration were unfruitful. The titration curve suggested one deprotonation event, but the amount of NaOH added (2 equivalents) clearly indicated that both deprotonation events had occurred. That is to say that the two values are very close. Given an order of magnitude difference in k_{obs} at pH 1.5 and pH 3.7 in Figure 3b one can assume that k_{2a} and k_{2c} are similar for the sake of estimating minimum and maximum values for pKa_1 and pKa_2. If all MA is in the form MAH^- at the apex, then the pKa is at the midpoint on each side of the apex in Figure S3. Therefore, $2.8 \leq pKa_1 \leq 3.7$ and $3.7 \leq pKa_2 \leq 4.4$ for *ct*MA at 90 °C. With these ranges in mind, a simplified model was constructed by initially viewing the system from the two extremes (low pH and high pH) in Excel, then simulations were iteratively carried out with KINSIM to fit the middle and obtain values for k_{1b} and k_{2b}. The equations are shown in eqs S11a & 11b. Analogous equations were used for *ct*MA. Equation S11c shows low pH estimates with the acid catalysed lactonisation pathway. An example fit is shown in Figure S4. Rate constants and equilibrium constants obtained from these fits were then entered into KINSIM software and plotted (stars in Figure S4) and maximum and minimum values for Ka_1, Ka_2 (for both *cc*MA and *ct*MA), k_{1b}, and k_{2b} are shown in Table S1. The ranges seem reasonable for all temperatures, however, there is more error in the estimates for 22.5°C due to the relative asymmetry of the curve (Figure 3a in the manuscript). 50 and 83 °C transformations of *cc*MA had a profile more similar to Figure 3b. Enthalpy and entropy of activation were estimated for reactions k_{1b} and k_{2b} based on the order of magnitude for the range expressed in Table S1. The values obtained were 97 kj/mol and 106 kj/mol for k_{1b} and k_{2b} enthalpy of activation, respectively, and -16 j/molK and -52 j/molK for k_{1b} and k_{2b} entropy of activation, respectively.

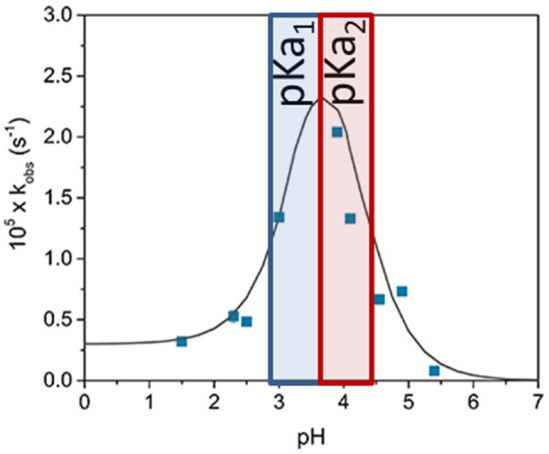

Figure S3. k_{obs} *vs* pH for lactonisation of ctMA at 90.0 °C.
The range of values for pKa_1 is shown in the blue box and for pKa_2 in the red box.

Derivation of the simplified model for Scheme 3 in the manuscript: Consider MAH_2/MAH^- and MAH^-/MA^{2-} as two separate systems:

$$K_{a1} = \frac{[MAH^-][H^+]}{[MAH_2]} \;\&\; [MA]_{total} = [MAH_2] + [MAH^-] \qquad \text{eq S9a}$$

$$\text{Therefore, } [MAH_2] = \frac{[H^+]}{[H^+] + K_{a1}} \times [MA]_{total} \;\;\&\;\; [MAH^-] = \frac{K_{a1}}{[H^+] + K_{a1}} \times [MA]_{total} \qquad \text{eq S9b}$$

$$Rate_{low\,pH} = k_{low\,pH} \times [MA]_{total} = ([MAH_2]k_{1a} + [MAH^-]k_{1b}) = \frac{[H^+]k_{1a} + K_{a1}k_{1b}}{[H^+] + K_{a1}} \times [MA]_{total} \qquad \text{eq S10}$$

$$k_{low\,pH} = \frac{[H^+]k_{1a} + K_{a1}k_{1b}}{[H^+] + K_{a1}} \qquad \text{eq S11a}$$

$$k_{high\,pH} = \frac{[H^+]k_{1b} + K_{a2}k_{1c}}{[H^+] + K_{a2}} \qquad \text{eq S11b}$$

$$k_{low\,pH + H^+\,Cat} = \frac{[H^+]([H^+] \times k_{2H} + k_{2a}) + K_{a1}k_{2b}}{[H^+] + K_{a1}} \qquad \text{eq S11c}$$

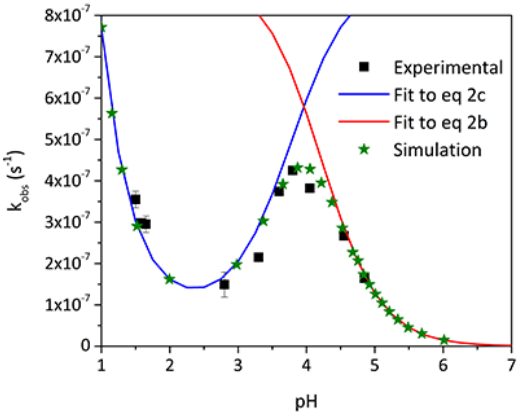

Figure S4. Fits of k_{obs} for *ct*MA conversion at 50 °C as a function of pH with high and low pH estimations in Excel (lines) and KINSIM (stars).

Table S1. Range of acid dissociation constants and rate constants k_{1b} and k_{2b} possible from simulations[a]

	22.5 °C[b]	50.0 °C	75.0 °C	83.3 °C	90.0 °C
*cc*MA					
pKa_1 range	2.8-4.4	3.6-4.1	-	3.2-4.0	-
pKa_2 range	4.2-5.0	4.1-4.8	-	4.0-4.6	-
k_{1b} range	$0.6\text{-}4 \times 10^{-5}$	$4\text{-}10 \times 10^{-4}$	-	$2\text{-}4 \times 10^{-2}$	-
*ct*MA					
pKa_1 range	-	3.2-3.7	3.8-4.5	-	2.8-3.7
pKa_2 range	-	3.7-4.8	4.5-5.0	-	3.7-4.4
k_{2b} range	-	$5\text{-}15 \times 10^{-7}$	$8\text{-}15 \times 10^{-6}$	-	$4\text{-}8 \times 10^{-5}$

[a] Elementary rate constants have the unit (s^{-1}). pKa ranges were identified as outlined above. [b] pKa range estimates at 22.5 °C are believed to be less accurate due to the relative asymmetry in the curve shown in Figure 3a. Higher temperatures were more symmetric with ~ a 10-fold difference in k_{obs} at the apex vs. low pH.

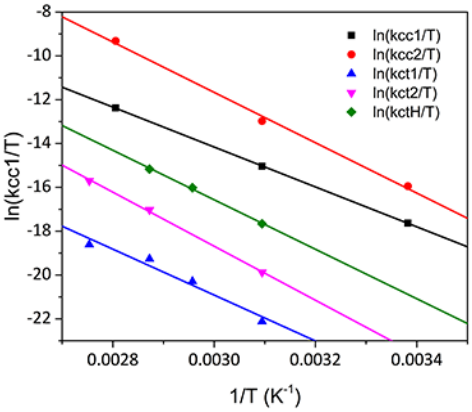

Figure S4. Plot of ln{(elementary rate constants in Table 1)/T} vs 1/T (eq 3).
Enthalpy of activation is derived from the slope and entropy of activation from the intercept.

The strong carboxylate/γ-C interaction in *ct*MA is easily observed by the changes in ^{1}H NMR chemical shift as a function of pH. Figure S5 shows a typical change in chemical shift with protonation state in acetic acid (ca. 0.2 ppm), and the unusually large changes observed on the γ-carbon relative to the *cis*-carboxylic acid moiety (0.8 ppm). The carbon α to the *cis*-carboxylic acid only changes by ~0.3 ppm.

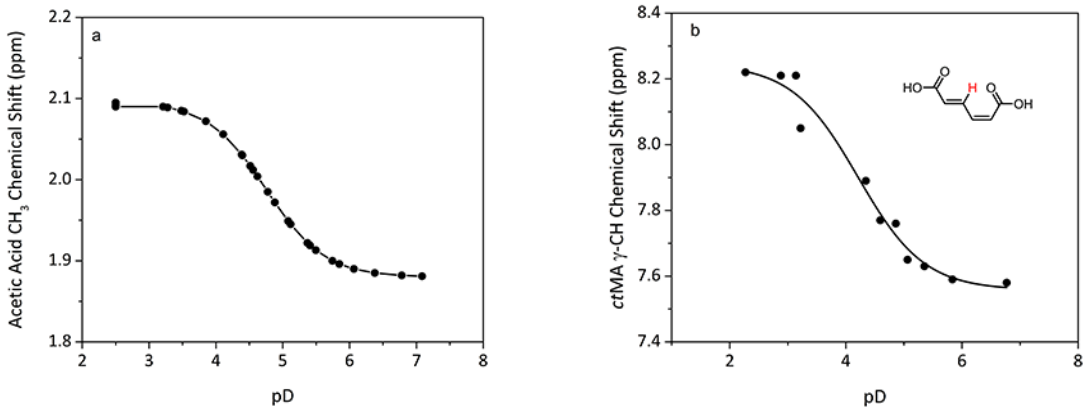

Figure S5. Experimentally determined changes in ^{1}H NMR chemical shift with simple protonation/deprotonation of acetic acid (a) and the strong intramolecular interaction observed by changes in chemical shift in *ct*MA (b). 600 MHz NMR, spectra acquired in D_2O at room temperature.

Lanthanum catalysed isomerisation sensitivity to pH

The lanthanum(III) catalysed isomerisation to *tt*MA is pH sensitive (Scheme S2). At low pH all *ct*MA is in the form *ct*MAH_2, and therefore cannot form a complex with La^{3+}. As pH is increased *ct*MA becomes deprotonated which facilitates La-O_2C-R^{2+} formation. However, further increases in pH will result in formation of $La(H_2O)_5OH^{2+}$ species which exhibit both lower solubility and smaller binding constants for carboxylate. The highest selectivity to *tt*MA (85%) was achieved near pH ~ 5 at 75 °C after 27 days. Mlac formation in parallel reaction pathways made up the other 15%.

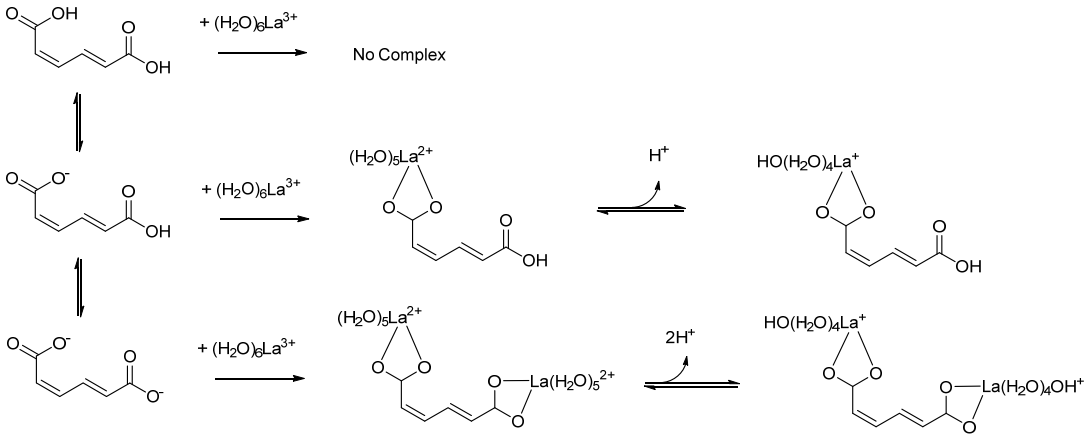

Scheme S2. Lanthanum catalysed isomerisation of *cc*MA to *tt*MA.

ttMA recovery and lanthanum catalyst recycling

Attempts to recover *tt*MA and recycle La(III) catalysts by taking advantage of the differences in solubility of $La(NO_3)_3$ and *tt*MA at low pH ($La(NO_3)_3$ solubility > 15000 × *tt*MA) were unsatisfactory. Only about 24% of the initial MA was recovered upon acidification and concentration by rotary evaporation. However, the recovered solid was exclusively in the form *tt*MA due to the differences in solubility of the 3 isomers at low pH (*cc*MA ~1g/L, *ct*MA = 5.2 g/L, and *tt*MA = 90 mg/L) [1]. The La(III) was precipitated by addition of NH_4OH then filtered. The recovered La salt, however, had a pale yellow color due to unrecovered MA and degradation products. Repeated MA and La recovery cycles resulted in only modest increases in MA recovery (an additional 0.5 – 1% per attempt). Never-the-less the lanthanum salts were redissolved in HNO_3 solutions containing fresh *cc*MA, pD was adjusted, and the solutions were heated to 90 °C an additional 6 – 8 days. Similar yields were achieved. A third attempt to recycle La salts was plagued by the unrecovered MA impurities which made balancing pD requirements with $(H_2O)_{4-n}La(OH)_n MAH_x^{+(3-n-x)}$ solubility difficult. Attempts to extract MA with ethyl acetate were somewhat more successful (*ca.* 60% MA recovered), but resulted in significant loses of La(III).

References

1. J. E. Matthiesen, J. M. Carraher, M. Vasiliu, D. A. Dixon and J.-P. Tessonnier, *ACS Sustainable Chemistry & Engineering*, 2016, **4**, 3575-3585.